Annual Report of U.S. Airforce Sponsered Project

AOARD AOARD-05-4093

Localized Synthesis of Silicon Nanocrystals in Silicon-rich SiO_2 by CO_2 Laser Annealing

Gong-Ru Lin[1, 2]

[1]Department of Photonics and Institute of Electro-Optical Engineering

National Chiao Tung University

1001, Ta Hsueh Road, Hsinchu, Taiwan 300, Republic of China

E-mail: grlin@faculty.nctu.edu.tw

[2]Graduate Institute of Electro-Optical Engineering

National University

1, Roosevelt Rd. Sec. 4, Taipei 106, Taiwan, Republic of China

E-mail: grlin@ntu.edu.tw

Abstract

The optical properties of a SiO_x film rapid-thermal-annealed (RTA) by CO_2 laser are primarily investigated. The micro-photoluminescence (μ-PL) and HRTEM analysis indicate that the precipitation of random-oriented Si nanocrystals can be initiated when laser intensity (P_{laser}) larger than 4.5 kW/cm^2. At P_{laser} of 6 kW/cm^2, the Si nanocrystals exhibits a largest diameter of 8 nm and a highest density of 4.5×10^{16} cm^{-3}, which emits strong PL at 790-825 nm. The micro-photoreflectance of the CO_2 laser RTA SiO_x film reveals a volume-density-product dependent refractive index increasing from 1.57 to 1.87 as the P_{laser} increases from 1.5 to 7.5 kW/cm^2. Nonetheless, the laser ablation of SiO_x film occurs with a linear ablation slope of 35 nm/kW/cm^2 at beyond 7.5 kW/cm^2, which terminates the enlargement of Si nanocrystals, degrades the near-infrared PL, and slightly reduces the refractive index of the CO_2 laser RTA SiO_x film.

Index Terms— CO2 Laser annealing, Si nanocrystal, SiOx, Nanotechnology, micro-photoluminescence.

I. Introduction

CO2 laser based zone annealing (or zone drawing) technique has previously emerged to modify the morphology or structural properties of different materials including polymers [1,

Report Documentation Page

Form Approved
OMB No. 0704-0188

1. REPORT DATE	2. REPORT TYPE	3. DATES COVERED
01 MAY 2007	**FInal**	**29-08-2005 to 28-08-2006**

4. TITLE AND SUBTITLE
Localized Synthesis of Silicon Nanocrystals in Silicon-rich SiO2 by CO2 Laser Annealing

5a. CONTRACT NUMBER
FA520905P0626

5b. GRANT NUMBER

5c. PROGRAM ELEMENT NUMBER

6. AUTHOR(S)
Gong-Ru Lin

5d. PROJECT NUMBER

5e. TASK NUMBER

5f. WORK UNIT NUMBER

7. PERFORMING ORGANIZATION NAME(S) AND ADDRESS(ES)
National Chiao Tung University,1001 Ta Hsueh Rd,Hsinchu 300 Taiwan,TW,300

8. PERFORMING ORGANIZATION REPORT NUMBER
N/A

9. SPONSORING/MONITORING AGENCY NAME(S) AND ADDRESS(ES)
AOARD, UNIT 45002, APO, AP, 96337-5002

10. SPONSOR/MONITOR'S ACRONYM(S)
AOARD

11. SPONSOR/MONITOR'S REPORT NUMBER(S)
AOARD-054093

12. DISTRIBUTION/AVAILABILITY STATEMENT
Approved for public release; distribution unlimited

13. SUPPLEMENTARY NOTES

14. ABSTRACT
The optical properties of a SiOx film rapid-thermal-annealed (RTA) by CO2 laser are primarily investigated. The micro-photoluminescence (-PL) and HRTEM analysis indicate that the precipitation of random-oriented Si nanocrystals can be initiated when laser intensity (Plaser) larger than 4.5 kW/cm2. At Plaser of 6 kW/cm2, the Si nanocrystals exhibits a largest diameter of 8 nm and a highest density of 4.51016 cm-3, which emits strong PL at 790-825 nm. The micro-photoreflectance of the CO2 laser RTA SiOx film reveals a volume-density-product dependent refractive index increasing from 1.57 to 1.87 as the Plaser increases from 1.5 to 7.5 kW/cm2. Nonetheless, the laser ablation of SiOx film occurs with a linear ablation slope of 35 nm/kW/cm2 at beyond 7.5 kW/cm2, which terminates the enlargement of Si nanocrystals, degrades the near-infrared PL, and slightly reduces the refractive index of the CO2 laser RTA SiOx film.

15. SUBJECT TERMS
Nanotechnology, CO2 Laser annealing, Si nanocrystal, SiOx, Nanotechnology, micro-photoluminescence

16. SECURITY CLASSIFICATION OF:			17. LIMITATION OF ABSTRACT	18. NUMBER OF PAGES	19a. NAME OF RESPONSIBLE PERSON
a. REPORT	b. ABSTRACT	c. THIS PAGE			
unclassified	**unclassified**	**unclassified**	**Same as Report (SAR)**	**13**	

2], metallic thin films [3-5], and superconductors [6], and dielectrics [7] etc. Particularly, such a laser heating process was also found to initiate the re-crystallization and sintering of ceramic powders [8], or to enhance the surface crystallinity and the specific phase of an optical nonlinear crystal (beta-BBO) [9]. Optical microscopy has shown that the crystallite surface exhibits same morphology as those observed after traditional furnace processing, however, the effect of CO2 laser annealing on the growth rate and the crystallite size is more pronounced. Not long ago, the CO2 laser annealing was primarily employed to improve the properties of a liquid-phase deposited, fluorinated silicon oxide film, which helps to concentrate the fluorinated silicon oxide film and reduce the effective surface charge density caused by surface defect states [7]. Nonetheless, the CO2 laser annealing induced modifications are intensity (Plaser) dependent and usually becomes prominent at Plaser >10 kW/cm2. Recently, the high-temperature (>1000oC) furnace annealing is employed to precipitate the Si nanocrystals in SiO2 film [10]. However, such a high-temperature heat treatment could seriously damages the whole integrated circuits (ICs) on the same Si wafer, which constrains the monolithic integration of the Si nanocrystal doped SiOx layer with the Si based ICs. Owing to the large absorption coefficient as high as 1.2×103 cm-1 of the oxide material at wavelength of 10.6 μm, a CO2 laser annealing of SiOx film on quartz substrate is investigated for the first time. In this letter, the optical properties and the size/density of localized precipitated Si nanocrystals embedded in the CO2-laser rapid-thermal-annealed (RTA) SiOx film are analyzed by high resolution transmission electron microscopy (HRTEM), micro-photoluminescence (μ-PL) and micro-photoreflectance (μ-PR).

II. Experimental

The 280-nm thick SiO_x films were deposited on both-side polished quartz substrates by using high-density plasma enhanced chemical vapor deposition (PECVD) with a gas mixture of SiH_4 and N_2O. The substrate-temperature was kept at 150 ^{o}C for 15 min to balance the temperature of the quartz substrate before deposition. The fluence ratio of SiH_4 to N_2O, the rf power and the reaction gas pressure were 1:6, 50 W and 120 mTorr, respectively. Afterwards, the CO_2 laser RTA was performed in atmosphere using a CW CO_2 laser (LTT Corp., ILS-II with a maximum power of 30 W) with P_{laser} ranging from 1.5 to 13.5 kW/cm^2. The laser spot was focused within 0.2 mm^2 using a hemispherical lens. The CO_2 laser illuminating time was as short as 1 ms. The ablation thickness of SiO_x film was measured

by α-step with a resolution of 1 nm. The μ-PL (or μ-PR) of CO_2 laser RTA SiO_x pumped by a HeCd laser at 5 W/cm^2 and 325 nm was detected by a fluorescence spectrophotometer (Jobin Yvon, TRIAX-320). The μ-PR analysis is demonstrated using a similar system with a HeNe laser at wavelength and power of 632.8 nm and 2 mW, respectively. A HRTEM (JEOL, 4000EX TEM) with a point-to-point resolution of 0.17 nm was used to characterize the orientation, lattice constant, size and density of the precipitated Si nanocrystals in SiO_x film.

III. Results and Discussions

III-1. Surface Temperature Evaluation

The surface temperature ($T_{surface}$) of the SiO_x film under CO_2 laser RTA process was determined using a previously developed thermal-physical model [11-13]. Neglecting the heat transport due to convection, the thermal radiation and thermal expansion, the absorbed thermal energy per unit volume and per unit time of the SiO_x film annealed using a CO_2 laser with a Gaussian-like power envelope can be described as $g_{laser}(r, z) = 4P_{laser}(1\text{-}R)\exp(-4r^2/D^2)\exp(-\alpha z)/\pi D^2\ d_{absorb}$ [11], where P_{laser} is the illuminating intensity of the CO_2 laser, R is the optical reflectivity of $R=[(n\text{-}1)^2+k^2]/[(n+1)^2+k^2]$, r is the distance to the center of the focused laser spot, D is the beam diameter at 1/e intensity of the Gaussian distribution, α is the optical absorption coefficient of the SiO_x film, ($\alpha = 4\pi k/\lambda$), λ is the laser wavelength, d_{absorb} is the penetrating depth of the CO_2 laser. The real (n) and imaginary (k) parts of the refractive index of the SiO_x film at the wavelength of 10.6 μm in the room temperature are approximately 2.224 and 0.102, respectively. As a result, the temperature $T(r, z)$ and surface temperature $T_{surface}$ of the SiO_x film are expressed by the following equations [11, 12]:

$$T(r,z) = \frac{g_{Laser}(r,z)\,\tau}{\rho C_p} = \frac{4(1-R)}{\rho C_p} \times \frac{P_{Laser}\,\tau}{\pi D^2 d_{absorb}} \times \exp\left(\frac{-4r^2}{D^2}\right) \times \exp(-\alpha |z|) \qquad (1)$$

$$T_{surface}(r) = \frac{4(1-R)}{\rho C_p} \times \frac{P_{Laser}\,\tau}{\pi D^2 d_{absorb}} \times \exp\left(\frac{-4r^2}{D^2}\right) \qquad (2)$$

$$\frac{\partial T_{surface}(r)}{\partial r} = \left(\frac{-4r^2}{D^2}\right) \times \frac{4(1-R)}{\rho C_p} \times \frac{P_{Laser}\,\tau}{\pi D^2 d_{absorb}} \times \exp\left(\frac{-4r^2}{D^2}\right),\ r \quad 0 \qquad (3)$$

where τ, ρ and C_p are the illuminating time, the density and the specific heat of the SiO_x film, respectively. The optical absorption coefficient (α), the optical reflectivity (R), the Gaussian beam diameter at 1/e intensity (D), the radial distance (r), the illumination time (τ), the density (ρ), and the specific heat (C_p) of the SiO_x film are set as 1209 cm^{-1}, 0.145, 370 μm,

21 μm, 1 ms, 2800 kg/m^3 and 1270 J/kg/K, respectively. According to these parameters, the simulated $T_{surface}$ of the SiO_x film can be increasing from 130 ^oC and 3350 ^oC as the CO_2 laser P_{laser} enlarges from 1.5 to 13.5 kW/cm^2. Therefore, the $T_{surface}$ of the SiO_x film proportional to the CO_2 laser P_{laser} is estimated from Eq. (2). For example, the SiO_x surface temperature profile around the annealed zone under illuminating with the P_{laser} of 6 kW/cm^2 is shown in Fig. 1. The surface temperature at the central part of a Gaussian-beam illuminated zone is about 1349^{o}C. The temperature gradient around the annealed zone of the SiO_x film is also plotted in Fig. 1. Within an illuminating spot of 400μm diameter, the maximum temperature gradient is only 4.5 ^{o}C/μm.

III-2. HRTEM Analysis

As a result, the simulated $T_{surface}$ of the SiO_x film can be increasing from 130 ^oC and 3350 ^oC as the CO_2 laser P_{laser} enlarges from 1.5 to 13.5 kW/cm^2. At P_{laser} = 5.8 kW/cm^2 (or $T_{surface}$ = 1285 ^{o}C), the cross-sectional HRTEM image reveals that the diameters of Si nanocrystals precipitated in the SiO_x matrix are ranging from 3 nm to 8 nm, as shown in Fig. 2. The orientation of Si nanocrystals embedded in the SiO_x film is random, including the (111)-orientation with a lattice spacing of about 0.32 nm, as shown in the inset of Fig. 2. The HRTEM estimated density of the Si nanocrystals in the CO_2 laser RTA SiO_x film at P_{laser} = 5.8 kW/cm^2 is about 4.5×10^{16} cm^{-3}. Similar laser re-crystallization was previously demonstrated by using a tightly focused continuous-wave Ar^+ laser (λ = 514.5 nm) [14], which helps to synthesize Si nanocrystals in the hydrogenated amorphous SiO_x (a-SiO_x:H) film. It was found that the diameter of the Si nanocrystals increases from 2.5 to 12 nm under an extremely high P_{laser} of ranging from 600 kW/cm^2 to 2.6 MW/cm^2. However, the surface damage of the a-SiO_x:H film was also evidenced at such high intensities even with a short irradiating time. A latter experiment showed similar results by using a frequency-tripled Nd:YAG laser at wavelength and pulsewidth of 355 nm and 8 ns, respectively [15]. By increasing the peak energy density of Nd:YAG laser up to 350 mJ/cm^2, the size of Si nanocrystals can be enlarged to 200 nm. Such a process exhibits a similar surface damage problem since the peak P_{laser} of 4.4 MW/cm^2 on the sample surface is far beyond the ablation threshold. Gallas *et al*. [16] then observed that the threshold energy density of a 248 nm-KrF pulsed excimer laser for annealing SiO_x without any ablation is only 85 mJ/cm^2. Nonetheless, only a few Si nanocrystals can be precipitated in SiO_x under such low P_{laser}, since few laser energies are absorbed and transferred to heat by the SiO_x film with infinitely

small absorption coefficient of at such short wavelengths (for example, $\alpha < 1\times10^{-6}$ cm^{-1} at <532 nm) [13]. In contrast, the CO_2 laser crystallization can precipitate Si nanocrystals at a P_{laser} of at least 2 orders of magnitude smaller than that required for visible or UV lasers, which simultaneously eliminates the laser-ablation induced surface damage effect. The phase separation between Si and oxygen atoms can be initiated when sufficient energy is absorbed by the SiO_x film, however, the annealing temperature for the precipitation of Si nanocrystals should be higher than 900°C. Nesheva *et al*. [17] have observed the formation of amorphous Si nanoparticles in films annealed at 700°C for 1 h. To format the crystallite Si nanocrystals in SiO_x films, a furnace annealing at 1030°C for 1 h is mandatory, as confirmed by Raman scattering analysis. In addition, Yi *et al*. [18] have also demonstrated that the amorphous Si clusters can be formatted at annealing temperature ranging between 300 and 900°C, but the crystallization of these amorphous Si clusters is only observed by annealing in a nitrogen atmosphere at >900°C for 1 h. That is, the annealing temperature of lower than <900°C could not activate the crystallization process for the amorphous Si clusters, even if the annealing duration is lengthened. Under CO_2 laser annealing, the surface temperature of the SiO_x film is dependent on the CO_2 laser intensity, the lower CO_2 laser intensity will reduce the surface temperature of the SiO_x film. Our simulation has also interpreted a threshold annealing intensity of 4.5 kW/cm^2, which corresponds to a surface temperature of 1100°C for initiating the crystallization of the Si nanocrystals. Similarly, the Si nanocrystals are difficult to be precipitated and the size of the Si nanocrystals could not be larger at a lower CO_2 laser intensity even with longer exposure times.

III-3. μ-PL and μ-PR Analyses

Subsequently, the μ-PL and μ-PR are employed to characterize the localized optical properties of the CO_2 laser RTA SiO_x film. The power dependent μ-PL analysis reveals different luminescent features at annealing and ablation regions. The diameter and area of the CO_2 laser annealed zone are 500 μm and 0.2 mm^2, respectively. A tightly focused He-Cd laser beam, with a spot size much smaller than that of CO_2 laser zone, transverse scans across the CO_2 laser annealed SiO_x sample. In the outer area of the Gaussian laser spot, the SiO_x matrix is not re-crystallized and the Si nanocrystal is unable to be precipitated, since the P_{laser} as well as the equivalent $T_{surface}$ is relatively low. A broadband blue-green PL contributed by the radiative defects such as E'_δ centers [19] at 520 nm and the neutral oxygen vacancies centers [20] at 455 nm are observed (see Fig. 3). The PL peak red-shifts to 520

nm as P_{laser} slightly increases to 3 kW/cm^2 (equivalent to a surface temperature of 900 ^{o}C), indicating a more pronounced activation of the E'$_\delta$ defects than the oxygen vacancies (see the inset (b) of Fig. 3). Near the central region of the annealing spot, the precipitation of small-size Si nanocrystals (with a size of 0.8-1 nm) is initialized as the PL has further red-shifted to 600-620 nm at P_{laser} = 4.5 kW/cm^2 (or a corresponding surface temperature of 1100 ^{o}C). The average size of Si nanocrystals persistently enlarges as the significant PL at 806 nm with spectral width of 106 nm is obtained at P_{laser} = 5.8 kW/cm^2 (see the inset (d) of Fig. 3). The maximum PL peak wavelength is observed at 825 nm at P_{laser} = 7.5 kW/cm^2. Nonetheless, the density of Si nanocrystals in SiO_x also decreases at higher annealing laser intensities as the PL intensity at corresponding wavelength is greatly attenuated by an order of magnitude. The effect of P_{laser} on the laser ablation of the SiO_x film clearly shows a linear ablation slope of 35 nm/kW/cm^2 at P_{laser} beyond ablation threshold (6 kW/cm^2), as shown in Fig. 4. The corresponding temperature on the SiO_x surface is up to 1902 ^{o}C as P_{laser} becomes >7.5 kW/cm^2, which has already exceeded over the melting temperature of fused silica. Moreover, a CO_2 laser annealing process at P_{laser} >7.5 kW/cm^2 not only anneals the SiO_x film and precipitates Si nanocrystals locally, but also leads to an increasing of structural damage related PL at 410 nm by at least one order of magnitude. The SiO_x matrix could be promptly compressed during such a rapid laser ablation procedure, where numerous oxygen dependent defects such as weak-oxygen-bond (O-O) [21], oxygen vacancy and ionized oxygen molecule (O_2^-) [22, 23] with PL wavelengths at 410-455 nm are generated by the damaged bonds of the SiO_2 matrix (see the inset (f)-(g) of Fig. 3). Such a phenomenon was never observed in furnace annealed SiO_x film under a similar condition, as the furnace annealing usually causes a gradual recovery on the compressing strain of SiO_2 matrix nearby Si nanocrystals.

The refractive indices of CO_2 laser RTA SiO_x films measured by μ-PR are greatly increasing from 1.57 to 1.87 as P_{laser} increases from 1.5 to 7.5 kW/cm^2 (lower part of Fig. 5). The as-grown SiO_x deposited under a N_2O/SiH_4 flow ratio of 6 exhibits comparable refractive index with that reported by Ueno *et al*. [24]. The decrease in the N_2O/SiH_4 flow ratio from 7 to 0.2 leads to an increasing refractive index of SiO_x from 1.48 to 2.1. Such a variation is correlated with the precipitation of Si nanocrystals. At a surface temperature below 600 ^{o}C (or P_{laser} < 3 kW/cm^2), the change in refractive index is less than 0.6 % since the precipitation of Si nanocrystals has not yet been initiated. The refractive index of SiO_x reaches a maximum of 1.87 as the surface temperature increases to 1300 ^{o}C, while the average diameter

of Si nanocrystal is also largest. As an evidence, Parakash *et al*. [25] have previously demonstrated that the enlargement of Si nanocrystals can increase the refractive indices of the furnace-annealed PECVD-grown SiO_x film. The density of the Si nanocrystal is also increased under higher annealing temperature and longer annealing time. Similar refractive index was also observed for the Si-ion-implanted SiO_2 doped by Si nanocrystals with size of 1-3.5 nm [26]. Obviously, the more Si atoms segregate from the SiO_x matrix, the higher density of Si nanocrystals with uniform size can be obtained. From μ-PL, the precipitation of Si nanocrystals in the SiO_x film are initiated at P_{laser} >4.5 kW/cm^2 (or a corresponding surface temperature of 1100 ^{o}C), and the estimated size of Si nanocrystals is increased from 2.8 nm to 6 nm as P_{laser} increases from 4.5 to 7.5 kW/cm^2, as shown in upper part of Fig. 5. In contrast, the refractive indices of the CO_2 annealed SiO_x films slightly decreases from 1.87 to 1.79 as P_{laser} increases from 7.5 to 12 kW/cm^2. Further increasing P_{laser} not only increases the annealing temperature but also activates the segregation of Si atoms and increases the density of the Si nanocrystal concurrently. In this point of view, it is not appropriate to attribute the change in refractive index of SiO_x film only by the size variation of Si nanocrystals. From TEM analysis, it is observed that both the size of the Si nanocrystal is decreased when annealing the SiO_x films at P_{laser} >7.5 kW/cm^2 due to the re-oxidation of the Si nanocrystals. Moreover, the dramatically decreasing intensity of PL emitting from the Si nanocrystals also at higher annealing laser intensities corroborates well with a significant reduction in the density of the Si nanocrystals. This eventually results in an slightly decreasing value of the volume-density product for Si nanocrystals buried in the SiO_x, which evidently elucidate the effect of size and density of Si nanocrystals on the variation in refractive index or absorption coefficient of SiO_x films according to Mie theory [27]. Nonetheless, the effect of the dense oxygen dependent defects on the aforementioned optical constants should also take into account.

IV. Achievements and Conclusions

The structural and optical properties of the PECVD-grown Si-rich SiO_x film RTA by CO_2 laser are primarily characterized by using μ-PL, μ-PR and HRTEM in this work. The CO_2 laser RTA performs the *in-situ* and localized temperature control of the SiO_x film, which thus facilitates precipitating Si nanocrystals from damaging the nearby devices. The equivalent temperature of the SiO_x surface is increasing from 130 ^{o}C to 3350 ^{o}C as the CO_2 laser P_{laser} enlarges from 1.5 to 13.5 kW/cm^2. The Si nanocrystals with maximum diameter and density

of 8 nm and 4.5×10^{16} cm^{-3}, respectively, can be locally precipitated within the CO_2-laser RTA SiO_x film, giving rise to a near-infrared PL at 790-806 nm. These are obtained at just below ablation-threshold intensity (6 kW/cm^2), which is at least 2 orders of magnitude smaller than that required for visible or UV lasers. The power dependent μ-PL analysis indicates that the precipitation of small-size Si nanocrystals is initialized when P_{laser} > 4.5 kW/cm^2 and a maximum PL peak wavelength of 825 nm can be observed at P_{laser} = 7.5 kW/cm^2. Nonetheless, the SiO_x film is ablated with a linear ablation slope of 35 $nm/kW/cm^2$ at beyond threshold P_{laser} of 6 kW/cm^2. The μ-PR results indicate that the refractive index of the CO_2 laser RTA SiO_x film varies from 1.57 to 1.87 as the P_{laser} increases from 1.5 to 7.5 kW/cm^2. At the P_{laser} < 3 kW/cm^2, the change in refractive index is less than 0.6 % since the precipitation of Si nanocrystals has not yet been initiated. The refractive index of SiO_x reaches maximum as the surface temperature increases to 1285 ^{o}C, while the average diameter of Si nanocrystal is also the largest. Annealing at higher intensities not only damages the SiO_x structure, but also constrains the precipitation and Si nanocrystals and decreases the refractive index of the SiO_x. This eventually degrades the near-infrared PL and reduces the refractive index of the CO_2 laser RTA SiO_x film. With the support from US Air Force, three papers have been accepted to be published in international journals, and several papers were present in top international conferences, including on invited talk, as listed below.

Invited Talks:

[1] <u>Gong-Ru Lin</u>, "White-light and near-infrared electroluminescence of furnace or CO2 laser annealed Si-rich SiO2 with structural defects and Si nanocrystals", *2006 SPIE Symposium on Photonics Europe (PE 2006)*, paper 6195-32, Strasbourg, France, April 3-6, 2006.

[2] <u>Gong-Ru Lin</u>, "Retrospect on the Research of Silicon Nanocrystal Embedded Silicon Oxide Materials and Light-Emitting Devices in NCTU/IEO", *3rd Symposium on Nanophotonics Science and Technology*, Hwalian, Taiwan, September 13-17, 2005.

Journal papers:

[1] <u>Gong-Ru Lin</u>, Chun-Jung Lin, Yu-Lun Chueh, and Li-Jen Chou, "Localized CO_2 Laser Annealing Induced Dehydrogenation/Ablation and Optical Refinement of Si-Rich SiO_x Film with Embedded Si Nanocrystals", *Journal of Nanoscience and Nanotechnology*, in press, August 2006.

[2] <u>Gong-Ru Lin</u> and C.-J. Lin, "Micro Photoluminescence and Photoreflectence Analyses of

CO_2 Laser Rapid-Thermal-Annealed SiO_x Surface", *IEEE Transactions on Nanotechnology*, in press, August 2006.

[3] Chun-Jung Lin, Gong-Ru Lin, Yu-Lun Chueh, and Li-Jen Chou, "Analysis of Silicon Nanocrystals in Silicon-rich SiO_2 Synthesized by CO_2 Laser Annealing", *Electrochemical and Solid-State Letters*, Vol. 8, No. 12, pp. D43-D45, December 2005.

Conference Papers:

[1] Chun-Jung Lin, Gong-Ru Lin, Yu-Lun Chueh, and Li-Jen Chou, "Anomalous Absorption of Silicon Nanocrystals in Silicon-rich $SiO_{1.25}$ Matrix Precipitated by CO_2 Laser Annealing", *2006 Integrated Photonics Research and Applications (IPRA) and Nanophotonics (NANO) Topical Meeting*, Oral paper Nanomaterials NThC4, Uncasville, Connecticut USA, April 24-28, 2006.

[2] Gong-Ru Lin, "White-light and near-infrared electroluminescence of furnace or CO2 laser annealed Si-rich SiO2 with structural defects and Si nanocrystals", *2006 SPIE Symposium on Photonics Europe (PE 2006)*, paper 6195-32, Strasbourg, France, April 3-6, 2006.

[3] Chun-Jung Lin, Hao-Chung Kuo, and Gong-Ru Lin, "Analysis of silicon nanocrystals in silicon-rich SiO2 synthesized by CO2 laser annealing", *2005 Asia-Pacific Optical and Wireless Communications Conference and Exhibition (APOC 2005)*, oral paper 6020-72, Shanghai China, November 6-10, 2005.

V. Acknowledgements

The financial support by Asian Office of Aerospace Research and Development (AOARD), Detachment 2 of the Air Force Office of Scientific Research (AFOSR) under Contract No. FA5209-05-P-0626 AOARD-05-4093 is also acknowledged.

VI. References

[1] A. Suzuki and M. Ishihara, "Application of CO_2 laser heating zone drawing and zone annealing to Nylon 6 fibers," *J. Appl. Polym. Sci.*, vol. 83, pp. 1711-1716, 2002.

[2] A. Suzuki and T. Okano, "Zone drawing and zone annealing of Poly(ethyleneterephthalate) microfiber prepared by CO_2 laser thinning," *J. Appl. Polym. Sci.*, vol. 92, pp. 2989-2994, 2004.

[3] Q. He, M. H. Hong, W. M. Huang, T. C. Chong, Y. Q. Fu, and H. J. Du, "CO_2 laser annealing of sputtering deposited NiTi shape memory thin films," *J. Micromech. Microeng.*, vol. 14, pp. 950-956, 2004.

[4] H. C. Pan, C. C. Chou, and H. L. Tsai, "Low-temperature processing of sol-gel derived $La_{0.5}Sr_{0.5}MnO_3$ buffer electrode and $PbZr_{0.52}Ti_{0.48}O_3$ films using CO_2 laser annealing," *Appl. Phys. Lett.*, vol. 83, pp. 3156-3158, 2003.

[5] H. Gleskova, V. V. Ilchenko, V. A. Skryshevsky, and V. I. Strikha, "CO_2-laser annealing of Al/a-Si-H contact," *Czechoslovak J. Phys.*, vol. 43, pp. 169-178, 1993.

[6] V. S. Serbesov, P. A. Atanasov, and R. I. Tomov, "Modification of the properties of HTSC YBCO thin-films on Silicon by superfast laser annealing in oxygen with a CW CO_2-laser," *J. Mater. Sci.*, vol. 5, pp. 272-274, 1994.

[7] N. F. Wang, M. P. Houng, and Y. H. Wang, "CO_2 laser annealing on fluorinated silicon oxide films," *Jpn. J. Appl. Phys. Pt. 1*, vol. 38, pp. 5227-5231, 1999.

[8] S. Ono and Y. Masuo, "Crystallization and sintering of amorphous alumina powder by CO_2 laser irradiation," *J. Ceramic Soc. Jpn.*, vol. 112, pp. 577-580, 2004.

[9] A. F. Maciente, V. R. Mastelaro, A. L. Martinez, A. C. Hernandes, and C. A. C. Carneiro, "Surface crystallization of β-BaB_2O_4 phase using a CO_2 laser source," *J. Non-Crystal. Solids*, vol. 306, pp. 309-312, 2002.

[10]L. Pavesi, L. Dal Negro, C. Mazzoleni, G. Franzo, and F. Priolo, "Optical gain in silicon nanocrystals," Nature (London), vol. 408, pp. 440-444, 2000.

[11]J. Zhao, J. Sullivan, J. Zayac, and T. D. Bennett, "Structural modification of silica glass by laser scanning," *J. Appl. Phys.*, vol. 95, pp. 5475-5482, 2004.

[12]T. R. Shiu, C. P. Grigoropoulos, D. G. Cahill, and R. Greif, "Mechanism of bump formation on glass substrates during laser texturing," *J. Appl. Phys.*, vol. 86, pp. 1311-1316, 1999.

[13]E. D. Palik, *Handbook of Optical Constants of Solids* Orlando; New York: Academic Press, 1985, pp. 179-182.

[14]M. C. Rossi, S. Salvatori, F. Galluzzi, and G. Conte, "Laser-induced nanocrystalline silicon formation in a-SiO matrices," *Mater. Sci. Eng. B*, vol. 69, pp. 299-302, 2000.

[15]A. Janotta, Y. Dikce, M. Schmidt, C. Eisele, M. Stutzmann, M. Luysberg, and L. Houben, "Light-induced modification of a-SiOx II: Laser crystallization," *J. Appl. Phys.*, vol. 95, pp. 4060-4068, 2004.

[16]B. Gallas, C.-C. Kao, S. Fisson, G. Vuye, J. Rivory, Y. Bernard, and C. Belouet, "Laser annealing of SiOx thin films," *Appl. Surf. Sci.*, vol. 185, pp. 317-320, 2002.

[17]D. Nesheva, C. Raptis, A. Perakis, I. Bineva, Z. Aneva, Z. Levi, S. Alexandrova, and H. Hofmeister, *J. Appl. Phys.*, 92, 4678 (2002).

[18]L. X. Yi, J. Heitmann, R. Scholz and M. Zacharias, *J. Phys.: Condens. Matter*, 15, S2887

(2003).

[19]G.-R. Lin, C.-J. Lin, and C.-K. Lin, “Defect-enhanced photoconductive response of silicon-implanted borosilicate glass,” *Appl. Phys. Lett.*, vol. 85, pp. 935-937, 2004.

[20]H. Nishikawa, R. Nakamura, and J. H. Stathis, “Oxygen-deficient centers and excess Si in buried oxide using photoluminescence spectroscopy,” Phys. Rev. B, vol. 60, pp. 15910-15918, 1999.

[21]J. C. Cheang-Wong, A. Oliver, J. Roiz, and J. M. Hernanaez, “Optical properties of Ir^{2+}-implanted silica glass,” *Nucl. Instrum. Methods Phys. Res. B*, vol. 175, pp. 490-494, 2001.

[22] C.-J. Lin and G.-R. Lin, *IEEE J. Quantum Electron*. 41, 441 (2005).

[23] J. C. Cheang-Wong, A. Oliver, J. Roiz, J. M. Hernánaez, L. Rodríguez-Fernández, J. G. Morales and A. Crespo-Sosa, *Nucl. Instrum. Methods Phys. Res. B* 175, 490 (2001).

[24]K. Ueno, T. Kikkawa, and K. Tokashiki, “Reactive ion etching of silicon oxynitride formed by plasma-enhanced chemical-vapor-deposition,” *J. Vac. Sci. Technol. B,* vol. 13, pp. 1447-1450, 1995.

[25]G. V. Prakash, M. Cazzanelli, Z. Gaburro, L. Pavesi, F. Iacona, G. Franzo, and F. Prilolo, “Linear and nonlinear optical properties of plasma-enhanced chemical-vapor deposition grown silicon nanocrystals,” *J. Modern Opt.*, vol. 49, pp. 719-730, 2002.

[26]A. E. Naciri, M. Mansour, L. Johann, J. J. Grob, and C. Eckert, “Correlation between silicon nanocrystalline size effect and spectroscopic ellipsometry responses,” *Thin Solid Films*, vol. 455-456, pp. 486-490, 2004.

[27]G. Mie, “Contribution on the optics of turbid media, especially colloidal metallic solutions,” *Ann. Phys.*, vol. 25, pp. 377-445, 1908.

VII. Figure Captions

Fig. 1. Surface temperature and temperature gradient in the annealing zone of SiO_x illuminated by CO_2 laser at P_{laser} = 6 kW/cm^2

Fig. 2. HRTEM cross-sectional image of the laser RTA SiO_x film by CO_2 laser at P_{laser} = 5.8 kW/cm^2.

Fig. 3. μ-PL spectra of CO_2 laser annealed SiO_x at different site of the annealed spot area.

Fig. 4. Laser ablated depth and normalized PL intensity of the laser RTA SiO_x film as a function of P_{laser}.

Fig. 5. The size of Si nanocrystal (upper part) and the refractive index of CO_2 laser RTA SiO_x film (lower part) at different laser intensities.

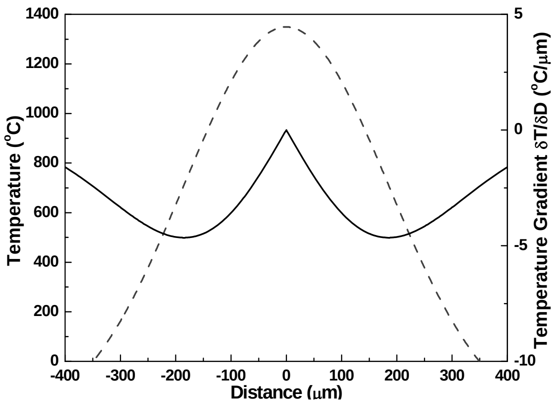

FIG. 1

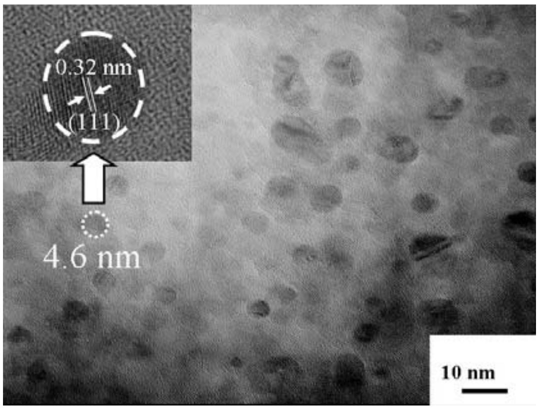

FIG. 2

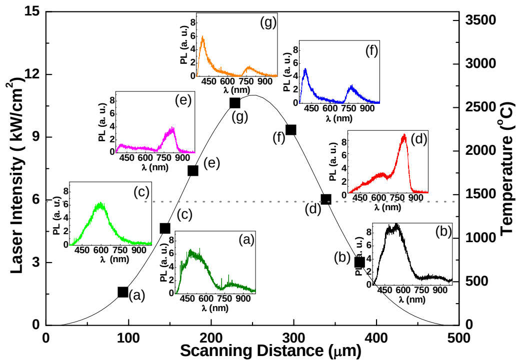

FIG. 3

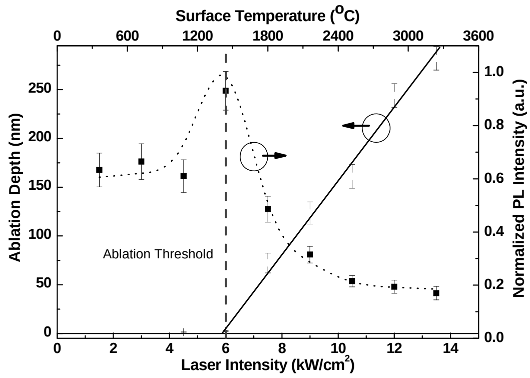

FIG. 4

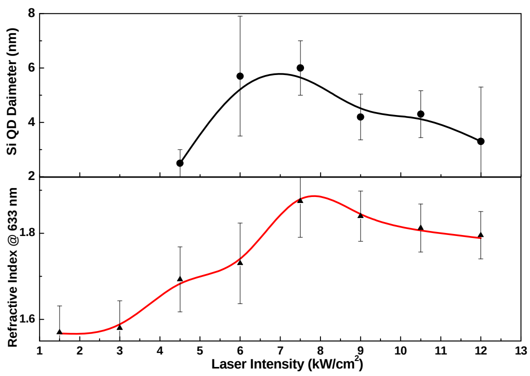

FIG. 5